

# Probing the contractile vacuole as Achilles' heel of the biotrophic grapevine pathogen *Plasmopara viticola*

Viktoria Tröster<sup>1</sup> · Tabea Setzer<sup>1</sup> · Thomas Hirth<sup>1</sup> · Anna Pecina<sup>1</sup> ·  
Andreas Kortekamp<sup>2</sup> · Peter Nick<sup>1</sup>

Received: 3 March 2017 / Accepted: 10 May 2017 / Published online: 26 May 2017  
© Springer-Verlag Wien 2017

**Abstract** The causative agent of Grapevine Downy Mildew, the oomycete *Plasmopara viticola*, poses a serious threat to viticulture. In the current work, the contractile vacuole of the zoospore is analysed as potential target for novel plant protection strategies. Using a combination of electron microscopy, spinning disc confocal microscopy, and video differential interference contrast microscopy, we have followed the genesis and dynamics of this vacuole required during the search for the stomata, when the non-walled zoospore is exposed to hypotonic conditions. This subcellular description was combined with a pharmacological study, where the functionality of the contractile vacuole was blocked by manipulation of actin, by Na, Cu, and Al ions or by inhibition of the NADPH oxidase. We further observe that RGD peptides (mimicking binding sites for integrins at the extracellular matrix) can inhibit the function of the contractile vacuole as well. Finally, we show that an extract from Chinese liquorice (*Glycyrrhiza uralensis*) proposed as biocontrol for Downy Mildews can efficiently induce zoospore burst and that this

activity depends on the activity of NADPH oxidase. The effect of the extract can be phenocopied by its major compound, glycyrrhizin, suggesting a mode of action for this biologically safe alternative to copper products.

**Keywords** Contractile vacuole · Downy Mildew · Glycyrrhizin · *Plasmopara viticola* · RGD peptides

## Introduction

*Plasmopara viticola* is the causative agent of Grapevine Downy Mildew, a severe disease in viticulture with tremendous economic impact worldwide. This parasitic protist belongs to the class of Oomycetes, organisms, which originally had been considered as fungi. As already pointed out in the famous textbook by Peter Sitte (Kleinig and Sitte 1986), phytopathological research during the second half of the last century has unequivocally demonstrated that the Oomycetes are not fungi (for a historical overview, see Kutschera and Hossfeld 2012). Meanwhile, these are classified into the phylum of biflagellate heterokont algae, the Stramenopila (Beakes et al. 2012). Distinct features are, for instance, their deviating ploidy (oomycetes are diplonts), and a cell wall composed of cellulose rather than chitin. The Oomycetes pass through a motile stage of their life cycle, where they harbour two differently shaped flagella. Native to North America, *P. viticola* has been accidentally introduced into Europe in the nineteenth century on grapevine root stocks used as biological control against the pathogenic insect *Phylloxera* (Gessler et al. 2011). Since the European Grape, *Vitis vinifera*, is a naïve host for *P. viticola*, the consequences were devastating: the pathogen rapidly conquered all European vineyards, and is now, in addition to Powdery Mildew, one major reason for the intense use of chemical plant protection (based on fungicides that are

---

This study is dedicated to the memory of Peter Sitte, Albert-Ludwigs-University of Freiburg, who passed away in 2016.

---

Handling Editor: Uli Kutschera

---

**Electronic supplementary material** The online version of this article (doi:10.1007/s00709-017-1123-y) contains supplementary material, which is available to authorized users.

---

✉ Peter Nick  
peter.nick@kit.edu

<sup>1</sup> Molecular Cell Biology, Botanical Institute Karlsruhe Institute of Technology (KIT), Fritz-Haber-Weg 4, Bld. 30.43, 76131 Karlsruhe, Germany

<sup>2</sup> Institute of Plant Protection State Education and Research Center (DLR) Rheinpfalz, Breitenweg 71, 67435 Neustadt, Germany

also used against true fungi) characteristic for conventional viticulture.

A central factor of this efficient spread is the high rates of fast asexual reproduction. After hibernation in old foliage or soil, the robustly armoured oospores initiate primary infection during spring rainfalls, and produce a germination peg terminating in a primary sporangium (Müller and Sleumer 1934). From here, rapid cycles of asexual propagation proceed on healthy grapevine organs, especially during humid and mild summer periods, resulting in epidemic spread all over the vineyard within few days. Numerous sporangia are produced and then transported by wind and rain drops. At high humidity, the sporangia release five to eight motile zoospores (Riemann et al. 2002) that swim towards the stomata of the host and start new infection cycles. Obviously, the success of the infection cycle depends on the efficiency by which the motile zoospore can sense and target the stomata (Kiefer et al. 2002). Zoospores accumulate at the stomata within several minutes and only in rare cases attach elsewhere. This stomatal targeting is impaired, when stomatal closure is induced by abscisic acid. Also, the subsequent steps of early pathogen development, such as germ-tube morphogenesis, seem to be coordinated by unknown signals from the host. These signals seem to be specific for the host species, because zoospores of *Plasmopara halstedii* (the causative agent for Sunflower Downy Mildew) did not target to stomata on grapevine leaves as efficiently as *P. viticola* (Kortekamp 2003).

Once the biflagellate zoospores have successfully located a stoma, they attach to the guard cells by means of adhesive mucus, shed their flagella, and encyst there. During encystation, zoospores undergo massive changes in structure: They round up, rapidly generate a cellulosic cell wall, eject the two flagella, and polarise their cytoskeleton (Riemann et al. 2002). After several hours, cysts germinate and produce a germination peg which reaches into the substomatal cavity. There, a substomatal vesicle is built from which a primary hypha emerges that penetrates into the mesophyll cells and forms haustoria to acquire nutrients from the host plant, without breaching the host membrane. The hyphae develop further into mycelia colonising the intercellular space of one intercostal field. At this stage, the infection can be seen with the naked eye as yellow “oil spots” on top of the leaves. After a few days, the mycelium develops sporangiophores that protrude through the stomata and form tree-like branched structures, which carry lemon-shaped sporangia. This sporulation is visible as whitish powder on the bottom side of the leaves inspiring the name of the disease (Downy Mildew). During humid conditions and night temperatures ranging between 16 and 23 °C, sporangia detach and are spread by wind and rain to start a new infection cycle (Müller and Sleumer, 1934). Zoospores can infect all green parts of vines including berries and inflorescences. Although Downy Mildew seems to be non-toxic for humans, it can cause allergic reactions

(Schaubschläger et al. 1994), and the losses in yield and quality by the resulting dry berries are substantial.

Control of Downy Mildew in the highly susceptible European grapevine species *V. vinifera* is difficult, since most of the life cycle proceeds inside the host. Traditionally, different copper compounds have been used, but since copper is toxic to many organisms and not only affects biological diversity in the soil but also poses a serious threat to the quality of ground water (reviewed in Van Zwieten et al. 2004), copper might be banned from conventional viticulture in the near future. However, copper preparations are still admitted for organic viticulture (up to 4 kg ha<sup>-1</sup> in Germany, and even up to 6 kg ha<sup>-1</sup> in France) with the argument that here no other alternatives for conventional fungicides are available. Nevertheless, this practice is seen progressively as problematic and a complete ban of copper products has been discussed since several years. Conventional fungicides against Downy Mildew include the strobilurins (Bartlett et al. 2002) and associated compounds belonging to the group of QoI fungicides. These compounds are doomed to failure, since already within 10 years of usage, *P. viticola* strains that have acquired resistance against these compounds have spread all over Europe (Chen et al. 2007), and there are even cases of multidrug resistance against all relevant groups of fungicides (Giraud et al. 2013). To increase the efficiency of fungicide applications and to confine further spread of fungicide resistance, interactive prediction systems, based on epidemiological, meteorological, and biological data, have been developed and successfully implemented (Bleyer et al. 2011).

As alternative to fungicides, new varieties have been generated by introgression of resistance loci from North American or Siberian grapes (Eibach et al. 2007). However, the initial success of this strategy is progressively endangered by the evolution of new strains of *P. viticola* that are able to overcome these resistances and as a result can infect even these resistant cultivars (Rouxel et al. 2013; Gómez-Zeledón et al. 2013).

These limitations in chemical or genetic control of Downy Mildew demonstrate that alternative targets are warranted. During most of its life cycle, the pathogen is well protected against fungicides, either because it is not accessible (hidden inside the host leaf) or because it is protected by cell walls, as in the case for sporangiophores, sporangia, and cysts. There exists only a very short phase in the life cycle, where the pathogen is really vulnerable: between hatching from the sporangium and the encystation at the stoma. This short phase represents something like the “Achilles’ Heel” of the pathogen and might be used as target for chemical plant protection. Zoospores provide at least two targets that are interesting: they need to locate the stomata, and they need to maintain their integrity during this mobile phase.

Stomatal targeting of mobile zoospores might contribute to differences of susceptibility between different grapevines as

concluded from a comparative infection study (Jürges et al. 2009) on grapevine species from North America, Asia and Europe. Whereas European species are successful colonised, species from North America and one species from Siberia can arrest the colonisation of *P. viticola* briefly after the formation of a germ tube. In several Asiatic species, a third response pattern was observed, where stomatal targeting was impaired. As a consequence, a small and aberrant mycelium was produced on the surface of the leaf that failed to infect successfully (Jürges et al. 2009). The fact that mistargeting of zoospores correlates with a failure of colonisation suggests that specific (host) signals control the interaction between host and pathogen. Chemotaxis of zoospores has also been reported for other Oomycetes, for instance, for the guiding of *Phytophthora cinnamomi* to the root (Allen and Newhook, 1973).

The second target is linked with the fact that zoospores lack cell walls. They are only protected by a cell membrane, making them as fragile as protoplasts. During a time interval of up to 30 min, zoospores are swimming unprotected over the leaf surface, and have to cope with a constant influx of water. During this period, they are probably attracted by plant substances released from the stomata. Only when they attach and encyst, they reacquire a cell wall that safeguards the cell against osmotic fluctuations. To avoid bursting, zoospores are endowed with contractile vacuoles, collecting water and expelling it in regularly cycles. Contractile vacuoles are pivotal for the regulation of cell volume and osmotic potential in freshwater protists (Patterson 1980). The contractile vacuole represents an interesting potential target for chemical plant protection, because this structure is only found in the Oomycete pathogen, but not in its plant host, such that it should be possible to find compounds that specifically inhibit the contractile vacuole while leaving the host cells untouched.

Nevertheless, knowledge about volume control of plant cells might contribute to understand also the physiology and regulation of the contractile vacuole. In fact, plant protoplasts as well, although lacking a contractile vacuole, are able to adjust cell volume to a certain extent in response to osmotic challenge by releasing or recycling membrane material from internal stores (Liu et al. 2013). This volume control is linked with a dynamic remodelling of submembraneous actin that, thus, must physically interact with the cell membrane and integrate mechanic load acting upon the membrane (reviewed in Nick 2011). Although plants lack canonical integrins that convey this function in mammalian cells, there seem to exist functional analogues. For instance, specific heptapeptides (YGRGDSP, usually referred to as RGD peptides) that can titrate the interaction of integrins with the extracellular matrix (reviewed in Ruoslahti 1996) are also effective in plant cells (Canut et al. 1998; Zaban et al. 2013). In addition to this functional analogy, there are structural analogies as well. A meshwork of adhesion sites at the plasma

membrane, termed the plasmalemmal reticulum (reviewed in Pickard 2008), shares morphological and molecular similarities with adhesion sites of mammalian cells and has been implicated with mechanosensory ion channels. Whether Oomycetes are endowed with a plasmalemmal reticulum is not known. However, the observation of fungal RGD-mediated adhesion (reviewed in Hostetter 2000) and specific effects of RGD peptides in *Achlya* and *Saprolegnia* (Chitcholtan and Garrill 2005; Kaminskyj and Heath 1995) indicates that functional integrin analogues also span the plasma membrane in Oomycetes and might integrate the extracellular matrix with intracellular actin.

The actin cytoskeleton of *P. viticola* is re-organised depending on stage, forming granulose plaque-like structures along with filaments in encysted and germinated spores, as well as longitudinal strands in germ tubes. Oomycete actin is strongly polarised not only at the site of germ tube emergence (*P. cinnamomi*, Hyde and Hardham 1993) but also within the germ tube itself (*P. viticola*, Riemann et al. 2002).

A participation of actin filaments and analogues or homologues of a plasmalemmal reticulum for the function of the contractile vacuole is likely, but the structural detection of these components in vivo is far from trivial, since the zoospores are moving vividly and are very small. However, it is possible to probe the functionality of the contractile vacuole by quantifying zoospore burst in response to compounds supposedly interfering with the plasmalemmal reticulum (RGD peptides) or apoplastic oxidative burst (Na, Cu, and Al ions) as important signal for osmosensing (reviewed in Ismail et al. 2014). These functional data of the contractile vacuole were combined with kinetic microscopy at high-resolution by both differential interference contrast, as well as after fluorescent visualisation of actin and endomembrane system. Using these approaches, the developmental sequence of the contractile vacuole was followed from its genesis during cellularisation of the syncytial sporangium till its disintegration upon encystment. To get insight into the membrane dynamics during cellularisation, different stages of sporangium germination till the hatching of zoospores were investigated by transmission electron microscopy leading to a model for mode of action for the traditional, copper-based control of Downy Mildew and, thus, also suggests the contractile vacuole as promising target for alternative, ecologically safer, ways of chemical control of this pathogen. We explore one of these alternatives: extracts from liquorice (*Glycyrrhiza spec.*) that have been reported to be effective against different Oomycete pathogens (Schuster et al. 2010). We can show that extracts from *Glycyrrhiza uralensis*, a plant used in Traditional Chinese Medicine, as well as the respective active compound, glycyrrhizin, efficiently induce zoospore burst and that this effect depends on the activity of NADPH oxidase, a membrane-based enzyme complex responsible for apoplastic oxidative burst.

## Material and methods

**Pathogen material** All observations were made with sporangia and zoospores of the plant pathogenic Oomycete *P. viticola* (Berk. & Curtis) Berl. & De Toni. To improve standardisation, strains derived from single sporangia were used (Gómez-Zeledón et al. 2013). These strains, 1191\_B11 and 1191\_B15, had been both collected from the host cultivar Lemberger in Lauffen, Germany and were kindly provided by the lab of Prof. Dr. Otmar Spring at Hohenheim University. The strains were propagated on excised leaves of the highly susceptible *vinifera* cultivar Müller-Thurgau. For inoculation, a fully expanded Müller-Thurgau leaf was placed with the lower surface on an aqueous suspension of mature sporangia ( $\sim 10^4$  sporangia  $\text{ml}^{-1}$ ) in a Petri dish of 14 cm in diameter and incubated overnight in the dark at 16 °C (Percival I-30 BLL, Percival Scientific, USA). The leaf was then removed from the suspension at the following day and transferred with the inoculated abaxial side turned upwards onto moist tissue in a fresh Petri dish further incubating with a cycle of 14 h light (TL-D Super 80 18W/840, Phillips, 25  $\mu\text{mol m}^{-2} \text{s}^{-1}$  according to Williams et al. 2007) and 10 h of night at a constant temperature of 16 °C. Under these conditions, the sporangia emerged after 4 days. Sporangia were harvested from dried leaves using a custom-built vacuum cleaner. For all experiments, only freshly harvested sporangia were employed.

**Visualisation of actin filaments** The spatial organisation of actin in *P. viticola* sporangia, phalloidin conjugated to Alexa Fluor 488 (Molecular Probes, Invitrogen), was followed after mild fixation according to the protocol of Riemann et al. (2002) with minor modifications. Five hundred microlitres of an aqueous zoospore suspension was fixed for 10 min in the same volume of a freshly prepared 2-fold fixation stock yielding a final concentration of 1.85% w/v paraformaldehyde in microfilament buffer (final concentration 100 mM  $\text{K}_2\text{HPO}_4$ , 100 mM  $\text{KH}_2\text{PO}_4$ , pH 7.3, 100 mM KCl, 0.25% Triton X-100). The sporangia were briefly spun down and washed twice with 1 ml of distilled water by carefully inverting the tube. After collecting the sporangia by a further centrifugation step, the supernatant was removed to a residual volume of 100  $\mu\text{l}$ , and the fluorescent phalloidin was added to a final concentration of 66 nM from a methanolic stock of 6.6  $\mu\text{M}$ . After staining for 10 min, the sporangia were observed by spinning disc confocal microscopy (details are given below) using an excitation at 488 nm line of an Argon-Krypton laser.

**Visualisation of ER** Endoplasmic reticulum (ER) and nuclear envelope in sporangia and zoospores of *P. viticola* were stained in vivo by 3,3'-dihexyloxa carbocyanine iodide (DiOC<sub>6</sub>, Molecular Probes, Invitrogen) according to Koning et al. (1993) with minor modifications. The dye was directly

added to a reaction tube with 1 ml of a zoospore suspension, released from around  $5 \times 10^4$  sporangia  $\text{ml}^{-1}$  and from a 10- $\mu\text{g ml}^{-1}$  stock in DMSO resulting in a final concentration of 10 ng  $\text{ml}^{-1}$  for the dye and 0.1% for the solvent (DMSO). Suspension and dye were mixed gently by inverting the tube and incubated for 30 min, before sporangia and zoospores were observed by spinning disc confocal microscopy under excitation with 488 nm (details are given below). Due to the incubation time, the sporangia were fully turgescient and some of them even exhibited active contractile vacuoles. Compared to the protocol of Koning et al. (1993) using yeast cells, the concentration of DiOC<sub>6</sub> was reduced by a factor of 1000, which was still perfectly sufficient to yield a good signal, but should minimise potential side effects of the dye on viability and physiology of the cells.

**Visualisation of endosomes** Endosomes were visualised by the polystyryl dye FM® 4-64 (Molecular Probes, Invitrogen) at a final concentration of 1  $\mu\text{M}$  added in the same manner to a sporangial suspension from a 1-mM stock solution. After incubation for 30 min, sporangia and zoospores were observed by spinning disc confocal microscopy under excitation with 561 nm (details are given below). Due to the incubation time, the sporangia were fully turgescient and some of them even exhibited active contractile vacuoles.

**Video microscopy of contractive vacuoles** Sporangia were collected from infected grapevine leaves with heavy sporulation by excising leaf discs of around 1  $\text{cm}^2$  that were transferred into 600  $\mu\text{l}$  of distilled water and inverted a few times to rinse off the sporangia. The donor leaf piece was then removed and the sporangia suspension incubated for 1–2 h in the dark at 16 °C in a phytotrone (I-30 BLL, Percival Scientific, USA), and the release of zoospores was monitored by checking aliquots microscopically. When the release was complete, 80  $\mu\text{l}$  of zoospore suspension was transferred to custom-made slides. These slides were wrapped twice with adhesive tape (tesa, Offenburg, Germany) in perpendicular direction to produce a central pool of 15 mm  $\times$  15 mm size and 1 mm depth which was important to prevent zoospore burst through the pressure exerted by the coverslip during observation. For video microscopy, the AxioImager.Z.1 microscope (Carl Zeiss, Jena, Germany) was used with a 63 $\times$  LCI- NeofluarImmCorr differential interference contrast (DIC) objective (NA 1.3) and the time-lapse mode of the camera (Axio-Cam MRm, Carl Zeiss, Jena, Germany) at a frequency of 4 Hz. Videos were analysed by the AxioVisionLE64 software (Carl Zeiss, Jena, Germany).

**Spinning disc confocal microscopy** Sporangia and zoospores stained by different fluorochromes to probe for actin, ER, and endosomes (see above) were viewed by spinning disc confocal microscopy (Zeiss, Jena, Germany) using a 63 $\times$ /1.44

DIC oil objective (Zeiss, Jena, Germany) and a spinning-disc device (YOKOGAWA CSU-X1 5000). Confocal z-stacks were collected with an AxioObserver.Z1 (Zeiss, Jena, Germany). For Alexa Fluor 488 phalloidin and DiOC<sub>6</sub>, the 488 nm, and for FM@ 4-64, the 561 nm line of an Ar-Kr laser were used. Emission was at 518 and 670 nm, respectively. Images were analysed with the Zeiss software (ZEN, blue edition, Zeiss, Jena, Germany).

**Transmission electron microscopy of sporangia** To follow ultrastructural changes of sporangia maturation, freshly harvested sporangia were incubated in water for 1 h in the dark and collected by a brief centrifugation step. The sediment was resuspended in 1.5 ml of 0.1 M cacodylate buffer, pH 7.2, and then fixed in 2.5% glutaraldehyde according to Heumann (1992) by a microwave-assisted fixation protocol, followed by secondary fixation in OsO<sub>4</sub>. After dehydration in an increasing ethanol series (30, 50, 70, 80, 90, 100% ethanol), specimens were embedded into Epon and sectioned by ultramicrotomy (Ultracut R, Leica, Bensheim, Germany) with a diamond knife (DiATOME, Hatfield, PA). Ultra-thin slides were placed on pioloform-coated grids and kept dry in a grid box. After staining with 10% methanolic uranyl acetate and lead citrate, samples were viewed by transmission electron microscopy at 80 kV (Zeiss 912).

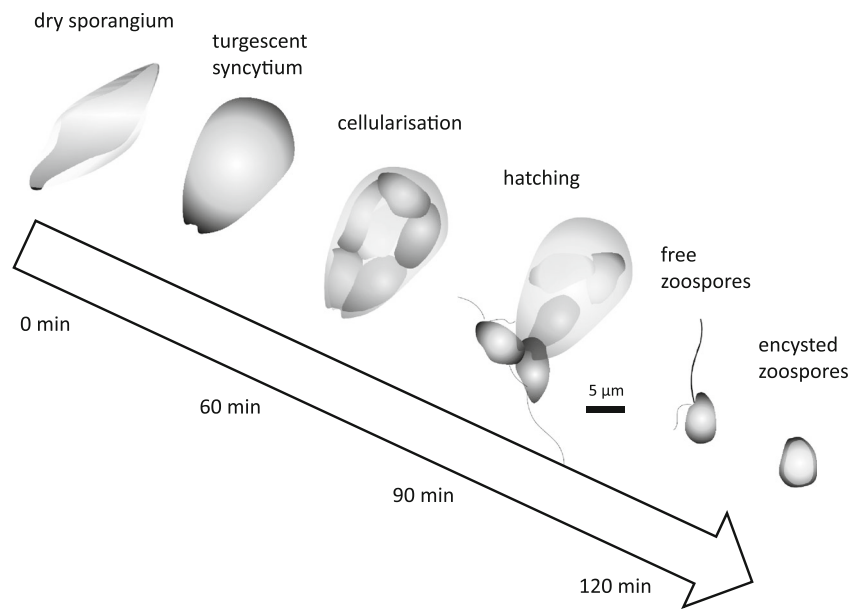
**Quantification of zoospore responses to different compounds** Mature sporangia were suspended to a concentration of  $1.5 \times 10^4$  sporangia ml<sup>-1</sup> in distilled water, and zoospores were allowed to hatch by incubation of the suspension in the dark at 16 °C for 1–2 h till the release of zoospores was complete, which was monitored by checking aliquots of the suspension by bright-field microscopy. The respective compound was then diluted directly into the suspension to the corresponding final concentration, and the suspension was then transferred into a haemocytometer (Fuchs-Rosenthal) and followed by differential interference contrast microscopy. Images of the observation field were recorded at regular time intervals over the following 90 min, and the incidence of zoospore burst was scored and related to the value observed at the same time point in a control experiment conducted in parallel with the same suspension, but without addition of this compound. In this control, no zoospore burst was observed up to 20 min, and also subsequently, only a low number of bursts were seen. The impact of low concentrations (up to 40 µM) of sodium chloride, copper sulphate, and aluminium chloride was tested, as well. To address a potential influence of the extracellular matrix, the specific heptapeptide YGRGDSP (RGD; Panatecs, Tübingen, Germany, purity >75%), mimicking the adhesive motives of animal fibronectin and vitronectin recognised by animal integrins (shown to interact with unknown plant analogues), and the inactive invert YGDGRSP (DGR; Panatecs, Tübingen, Germany, purity >75%) were

investigated along with the non-specific, charged peptide polyamine sulphate (Fluka, Buchs, Switzerland). The concentration of these peptides was varied, but never exceeded 50 ng ml<sup>-1</sup>. In some experiments, a commercial phytotherapeutic extract used for Traditional Chinese Medicine from *G. uralensis* (Nr. 118A, *Glycyrrhizae radix*, *Gan Cao*, PhÿtoComm®, Kehl, Germany) was used. The concentration of the active compound glycyrrhizin in this extract was estimated to range between 8 and 20 mg ml<sup>-1</sup> based on the typical values found in these roots (Chen and Sheu 1993, Yokozawa et al. 2000). Since the precise content of glycyrrhizin in this extract was not known, we also used the pure compound glycyrrhizin in some experiments (Roth, Karlsruhe, Germany) at 20 or 50 ng ml<sup>-1</sup>. The effect of glycyrrhizin was compared to the effect of either 250 nM of the actin polymerisation inhibitor Latrunculin B (Sigma, Deisenhofen, Germany), 250 nM of the membrane rigidifier dimethyl sulfoxide (DMSO, Roth, Karlsruhe, Germany), or 2 to 200 nM of diphenyleneiodonium (DPI, Sigma, Deisenhofen, Germany), a specific inhibitor of NADPH oxidases, respectively.

## Results

**Contractile vacuole activity precedes zoospore individuation** The mobile phase of the life cycle in *P. viticola* is very short (less than 2 h) and follows a developmental sequence of sporangial swelling; zoospore cellularisation; hatching; a mobile phase, where zoospores swim towards the stomata; and, as final point, attachment and encystation (Fig. 1). During this time interval, the cytoplasm experiences several sharp changes in water potential. To get insight into the cellular details of the transitions during sporangial swelling and zoospore individuation, we followed changes of ultrastructure by transmission electron microscopy after chemical fixation (Fig. 2). Whereas the dry sporangia shows a crinkled raisin-like shape (Fig. 2a), they immediately swell into lemon-shaped balloons (Fig. 2c) upon contact with water, indicating that the water potential of the cytoplasm in the dry sporangium must be very negative. Already prior to swelling, the cytoplasm is in close physical contact with the sporangial wall (Fig. 2b, spw), such that the increase in volume will build up a considerable turgor within a few seconds. The partitioning of the syncytial cytoplasm into individual zoospores prior to hatching (Fig. 1) requires that the cytoplasm has to detach from the sporangial wall (Fig. 2e, g), such that the turgor component of the water potential will return to zero, and this situation will persist throughout the entire mobile phase. Only when zoospores encyst and again generate their own individual cell wall (Fig. 1), the negative water potential of the cytoplasm will be again compensated by turgor pressure. These sharp changes of water potential are accompanied by dramatic

**Fig. 1** Schematic representation of early development between swelling of sporangia and encystation of zoospores. The time point of resuspending dry sporangia in water is defined as 0 min. Time points are average values for a host-free condition derived from Kiefer et al. (2002)



remodelling of the cytoplasm (Fig. 2). Prior to swelling, when the sporangial wall is still wrinkled (Fig. 2b, *spw*), numerous

small early dense-body vesicles (Fig. 2b, *edbv*) are observed. Their grey colour may indicate lipids, which have been

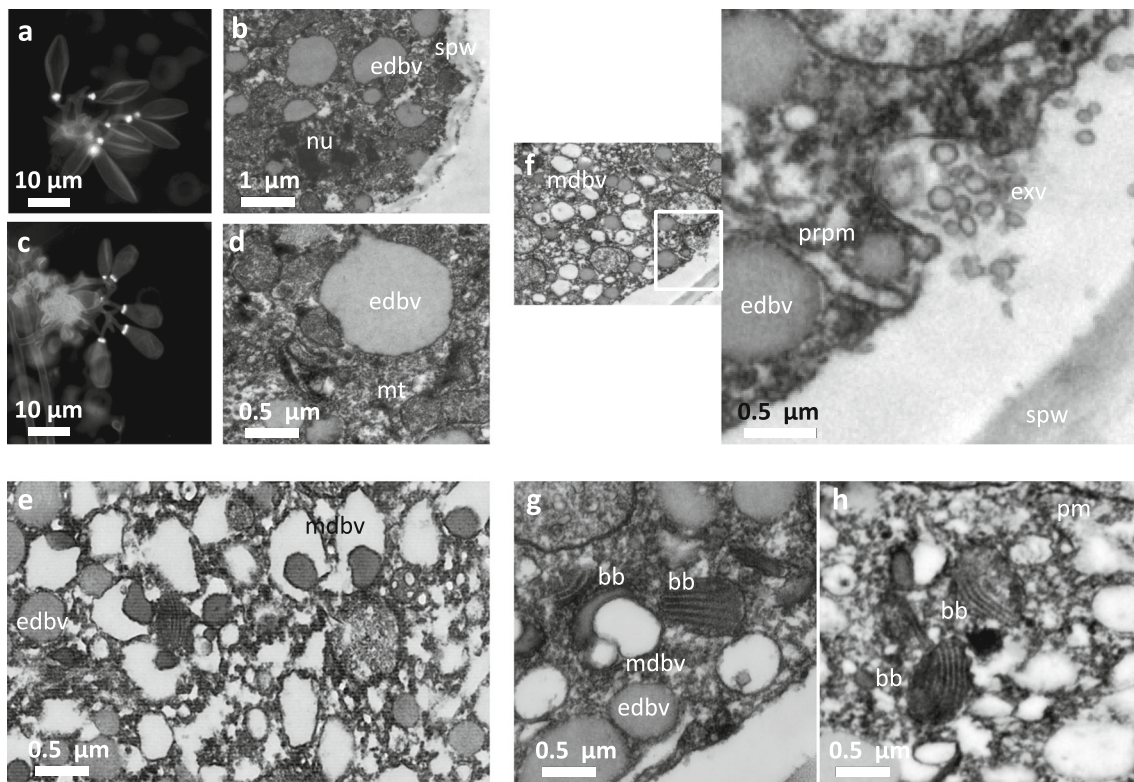


**Fig. 2** Ultrastructural details of sporangial swelling and zoospore individuation followed by transmission electron microscopy. Dry sporangia prior to swelling (**a**, **b**) in comparison with fully turgent sporangia (**c**, **d**) after aniline blue staining (**a**, **c**) and TEM (**b**, **d**) is compared to fully swollen sporangia; *nu* nucleus, *edbv* early dense-body vesicles, *mt* mitochondrion note the still wrinkled sporangial wall (*spw*) in **c**. **e** Emergence of numerous mature dense-body vesicles (*mdbv*) progressively replacing the early dense-body vesicles (*edbv*) in a

maturing sporangium. **f** Secretion of electron-dense material in a mature sporangium with partially completed separation of zoospores. *edbv* early dense-body vesicle, *prpm* prospective plasma membrane, *exv* exocytotic vacuole. Note that the zoospore has already detached from the sporangial wall (*spw*). **g**, **h** putative basal bodies (*bb*) in mature sporangia with almost completed individuation of zoospores; note the contiguous plasma membrane (*pm*) in **h**

proposed as energy source for the syncytium (Gay et al. 1971). These early dense-body vesicles are also seen in fully turgescient sporangia, but have increased in size and instead appear lighter in colour (Fig. 2d, edbv). Additional organelles, such as individual nuclei (Fig. 2b, nu) or mitochondria (Fig. 2d, mt), can be encountered as well. At later stages, the maturing sporangium contains numerous mature dense-body vesicles (Fig. 2e, f, mdbv), progressively emerging and replacing the grey early dense-body vesicles. Hereby, transitional stages can be encountered, where a smaller and denser structure that is clearly delineated by a membrane is seen inside a larger and white vesicle that is, by itself, lined by a membrane. With progressive maturation of the sporangium, a clear gap between sporangial wall and cell membrane develops (Fig. 2f, g), where granular material seems to be deposited by exocytotic vesicles (Fig. 2f, exv). Moreover, longer sheets lined by two membranes in parallel can be found that probably correspond to prospective plasma membranes between future zoospores in different stages of individuation (Fig. 2f, prpm; Fig. 2h, pm). Occasionally, pairs of oval structures with electron dense parallel stripes are encountered in some sections (Fig. 2g, h, bb), probably representing the basal bodies of the two flagella.

Sporangia are syncytial cells, containing several nuclei in the cytoplasm. We observed that contractile vacuoles were already active in the syncytial cytoplasm prior to cellularisation into single zoospores (Fig. 3a). A contraction cycle lasted around 30 s and comprised phases, where the vacuole was bifurcated followed by phases, where the two chambers fused to one larger vacuole (Fig. 3a, b). This sequence (lasting around

20–30 s) could be followed repeatedly, showing that the activity of contractile vacuoles starts prior to cellularisation of the syncytium. When this activity was investigated at high temporal resolution (4 frames per second), further details became observable: The bifurcated state persisted for the first 6 s (Fig. 3c (1–3)), starting with two vacuole chambers of comparable size (Fig. 3c (1)), followed by shrinkage of one chamber (Fig. 3c (2)), and fusion of both parts (Fig. 3c (3)) to a larger single vacuole (Fig. 3c (4)). This single vacuole was seen over the next 6 s (Fig. 3c (4–6)), but underwent phases of expansion and shrinkage (Fig. 3c (4, 6)), when it appeared rough and granular and dynamic, whereas the fully turgescient vacuole appeared translucent lined by a membrane that was clearly visible in the differential interference contrast (Fig. 3c (5)). Then, the next cycle started with the bifurcated initial situation (Fig. 3c (7)). Cellularisation proceeds by formation of membranes in a star-like manner in centrifugal direction (Fig. 3d). The cytoplasm is partitioned such that one contractile vacuole is assigned to each prospective zoospore.

**Contractile vacuole activity is linked with dynamic endomembrane remodelling** The structure of actin in turgescient syncytial sporangia was visualised by fluorescent phalloidin after mild chemical fixation (Fig. 4a). When subsequent sections from confocal z-stacks were followed, the mature sporangium was found to contain star-like, brightly fluorescent, actin plaques, from which connecting actin cables emanated, consistent with previous observations (Riemann et al. 2002). Whereas the fixation required to label actin by phalloidin did not allow to observe

**Fig. 3** Activity of contractile vacuole prior to cellularisation of the syncytium. **a, b** Mature sporangium with bifurcated contractile vacuole at the beginning (**a**) and end (**b**) of a recorded time-lapse series over 40 s. **c** Individual frames from a time-lapse series recorded at a frequency of 4 frames per second in the zoom-in indicated by the *white square* in **a** and **b**, time interval between the shown frames is 2 s. *White arrowheads* indicate the position of the contractile vacuole. **d** Two sporangia at incipient cellularisation, the ensuing cell membranes are indicated by *white arrows*; note the contractile vacuole in the upper sporangium (*white arrowhead*)

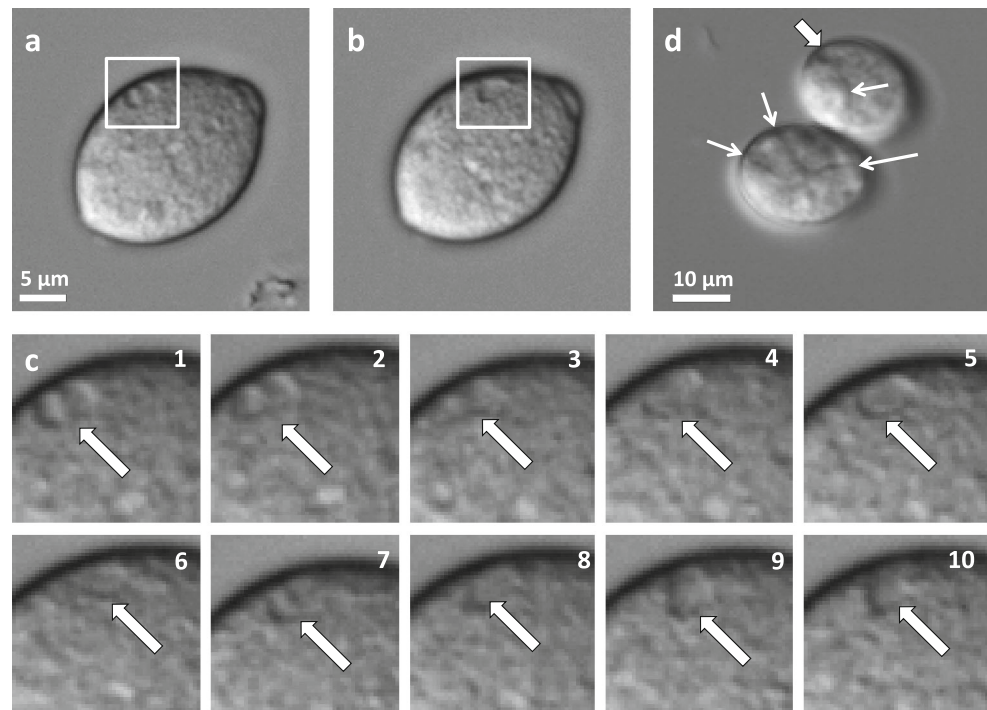
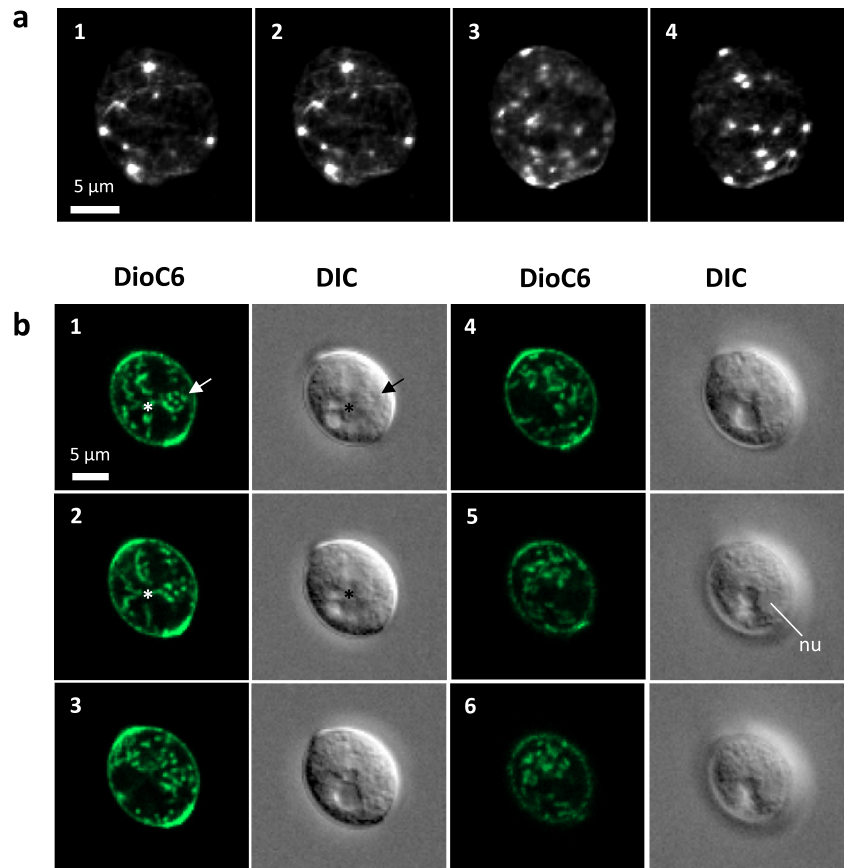


**Fig. 4** Cytology of the turgescing sporangium. **a** Actin visualised by fluorescent phalloidin after chemical fixation. Subsequent sections from a confocal z-stack. **b** ER visualised by DioC6 in vivo. Subsequent frames from a confocal section. The DioC6 signal is shown along with the corresponding image by differential interference contrast (DIC). *Arrows* indicate a release site of contractile vacuoles; *asterisks* indicate a star-like ER structure subtending the contractile vacuole. *nu* nucleus



potential dynamic changes nor the interrelation between the actin plaques with contractile vacuoles, it was possible to follow the endoplasmic reticulum (ER) in vivo using the fluorescent dye DiOC<sub>6</sub> (Fig. 4b, supplemental movie S2). This allows to see details of the contractile vacuole in the prehatching sporangium that would be hard to pick up in the rapidly moving zoospores. When the fluorescent DiOC<sub>6</sub> signal in individual sections from a confocal z-stack was followed over time in comparison with the corresponding image collected by differential interference contrast (DIC), two prominent arrays were observed during the phase, when the contractile vacuole was rough and granular (Fig. 4 (b1, b2)): A star-like ER structure (asterisks in Fig. 4 (b1, b2)) consisting of converging, multiple, ER cisternae separated the chambers of the contractile vacuole, and disappeared upon fusion of the chambers. Rosette-like structures composed of a central small cavity surrounded by several smaller or larger cavities were seen around the site of release (arrows in Fig. 4 (b1)) and would fuse with one ray of the ER star during the same phase (arrows in Fig. 4 (b1, b2)). During the subsequent phase of the contractile cycle, when the vacuole appeared smooth and translucent, the ER did not exhibit a pattern that was obviously linked with the contractile vacuole. It should be mentioned that the fluorescent signal appeared to be especially strong at the poles of the sporangium.

After individuation, the individual zoospores were already motile within a sporangium and were swimming actively even prior to hatching (Fig. 5a; the time interval between the frames 1–8 was 250 ms). Upon staining with the membrane impermeable endocytosis tracker FM4-64, the cell interior was strongly stained within a few minutes indicating a high intensity of endocytotic uptake (Fig. 5b). This was also observed for the mature, but still syncytial sporangium. Already in the prehatching state, the individual zoospores showed active contractile vacuoles. In the free zoospores, the contractile vacuole was observed in proximity of the flagellar roots (Fig. 5c).

To characterise functional and cytological aspects of contractile vacuoles of *P. viticola*, single zoospores were followed on their way by video microscopy and time series were recorded by differential interference contrast (shown representatively in Fig. 6a; Supplemental Movie S2). The entire cycle lasted around 3 s (mean value 3.28 s, standard error of the mean of 0.24 s,  $n = 42$ ) and, thus, was strongly (by around 10-fold) accelerated over the situation in the mature sporangium. The contractile vacuole was established during the first ~20% of the cycle, remained stable till ~90% of the cycle, and was then rapidly released during the last ~10% of the cycle. During the granular phase of the cycle, numerous vesicles could be seen to merge with the vacuole, but were replaced by radial channels in the translucent phase. These channels were dynamic as well, and persisted only a short time

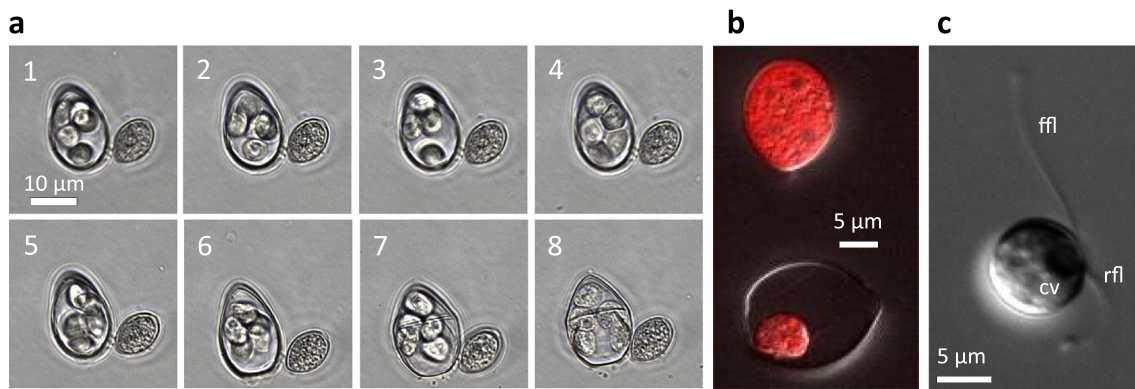


**Fig. 5** Cytology of zoospores. **a** Zoospores are released from turgor prior to hatching. **b** Intensive staining of syncytial sporangium (upper cell) and hatching zoospore (lower cell) by the endocytosis tracker FM® 4-64. **c**

Mobile zoospore recorded by differential interference contrast. *ffl* front flagellum, *rfl* rear flagellum, *cv* contractile vacuole

after emergence. Assuming a spherical shape for both vacuole and cell, the mean volume flow per second was estimated to be 3.8% ( $\pm 0.30\%$ ) of total volume, which means that in around 25 cycles (around 75 s), one entire cell volume of water must be secreted to prevent the zoospore from bursting.

**Contractile vacuole activity can be blocked by  $\text{Cu}^{2+}$ , by  $\text{Al}^{3+}$ , and by RGD peptides** Due to the massive secretion of water necessary to preserve integrity of a motile zoospore, even minor perturbation of the contractile vacuole is expected

to result in zoospore burst. The incidence of zoospore burst in response to different compounds can therefore be used as readout for the effect of these compounds on the functionality of the contractile vacuole. Under control conditions, no zoospore burst was observed up to 20 min; from 30 min, a low number (200 cases in a total population of around 120,000) could be observed at 30 min, and this value increased to 400 at 90 min. The variability in this number between biological replicas was 21%. Addition of 10  $\mu\text{M}$  of sodium chloride increased the incidence of zoospore burst by a factor of 4

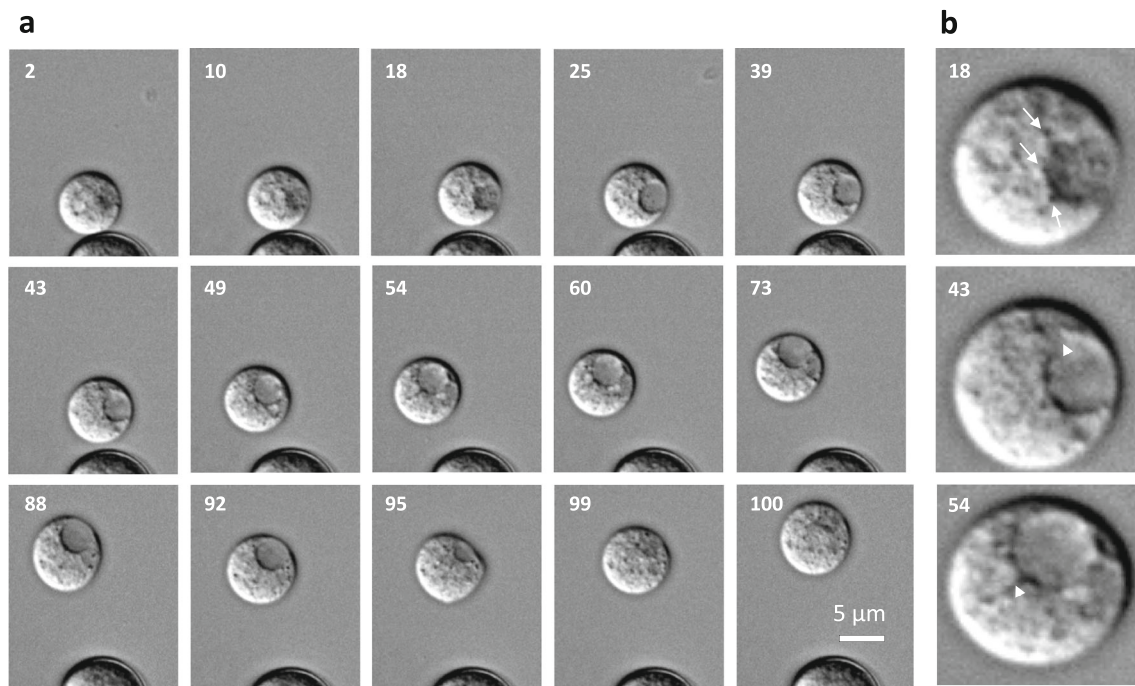


**Fig. 6** Functional and cytological details of the contractile vacuole in a free zoospore. **a** Time series over one contraction cycle recorded by differential interference contrast. The entire cycle lasted 3 s; *numbers* indicate the relative time of the respective frame in percent of the entire cycle (100% corresponding to one completed cycle). The contractile vacuole is established during the first ~20% of the cycle, remains stable till ~90% of the cycle, and is then rapidly released during the last ~10% of

the cycle. **b** Magnification of the contractile vacuole from the time series shown in **a** to highlight cytological details. *Numbers* as in **a**. *White arrows* indicate vesicular structures that fuse during the early phase of the contractile cycle, *white arrowheads* indicate channels of changing width that appear and disappear during the stable phase of the contractile cycle

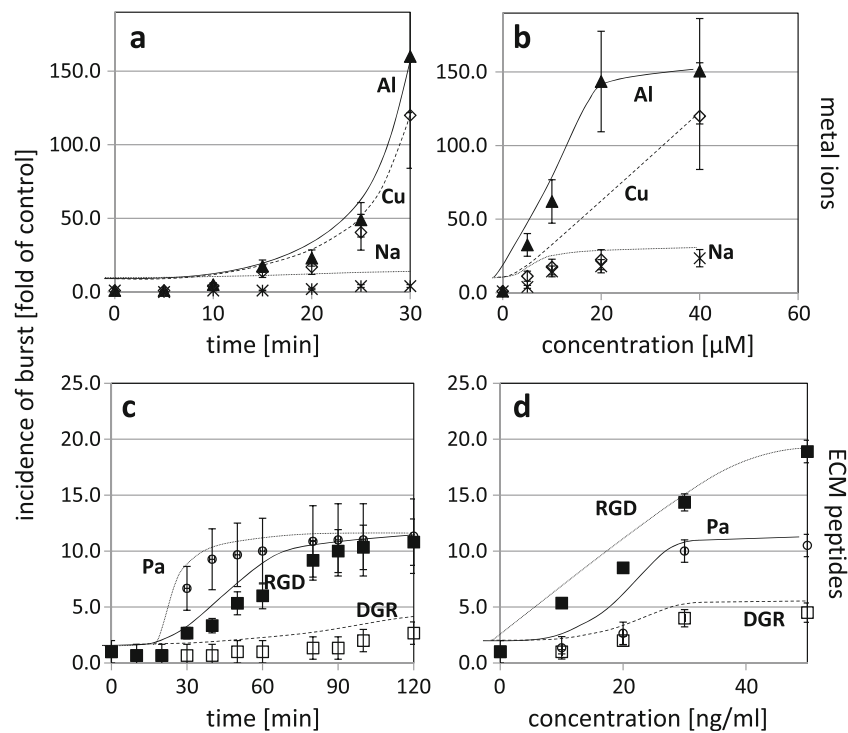


**Fig. 7** Chemical manipulation of zoospore burst. Metal ion (a, b), peptides interacting with the extracellular matrix (c, d), compounds act on actin, membrane fluidity, and generation of superoxide (e) have been tested, as well as an extract of *Glycyrrhiza uralensis*, a plant used in Traditional Chinese Medicine (f). The incidence of zoospore burst as readout for impaired function of the contractile vacuole is shown in relative values over a control without treatment. Time courses (a, c) and dose-response curves for a fixed time of treatment (b, d) are shown. As metal ions (a, b), aluminium (Al), copper (Cu), and sodium (Na) were tested, as peptides interacting with the extracellular matrix (ECM), the heptapeptide YGRGDSP (RGD) mimicking the adhesive motives of animal fibronectin and vitronectin recognised by animal integrins (shown to interact with unknown plant analogues), and the inactive invert YGDGRSP (DGR) were tested along with the non-specific, charged peptide polyamine sulphate. Time courses for metal ions (a) were recorded

(Fig. 7a). In contrast, addition of the same concentration of either copper sulphate or aluminium chloride drastically enhanced the incidence of zoospore burst to more than two orders of magnitude within 30 min compared to the control. A dose-response curve recorded at 30 min after the onset of the treatment (Fig. 7b) showed that the effect was saturated from 20  $\mu\text{M}$  in case of aluminium ions, whereas in case of copper, similar values were reached for 40  $\mu\text{M}$ . For sodium, from 20  $\mu\text{M}$ , a plateau at around 25-fold increase compared to the plateau was observed.

In animal cells, the heptapeptide YGRGDSP (abbreviated as RGD) is found in the extracellular matrix proteins fibronectin and vitronectin, and is recognised by animal integrins. The binding confers mutual adhesion between animal cells or their interaction with the extracellular matrix. To test whether analogues of integrins are relevant for the function of the contractile vacuole, the influence of RGD peptides was tested along with the biologically inactive, but equally charged invert YGDGRSP

for a concentration adjusted to 10  $\mu\text{M}$ ; in case of ECM-interacting peptides (c), the concentration was adjusted to 20  $\text{ng ml}^{-1}$ . Dose-response curves for metal ions (b) were measured at 30 min after addition of the ions, in case of ECM-interacting peptides (d), at 90 min after addition of the peptides. Identical concentrations of sporangia ( $15,000 \text{ ml}^{-1}$ ) were used, and each experiment was accompanied by an untreated control as internal standard. Values give the incidence of bursting zoospores relative to this internal standard at the final time point of the experiment (30 min in case of metal ions, 90 min in case of ECM-interacting peptides). Values represent means and standard errors from two independent experimental series; under control conditions, no zoospore burst was observed up to 20 min, a low number ( $200 \text{ ml}^{-1}$  of sporangial suspension) was observed at 30 min, and this value increased to  $400 \text{ ml}^{-1}$  at 90 min. The variability in this number between biological replicas was 21%

(DGR), and the non-specific, charged peptide polyamine sulphate. Time-courses of zoospore burst were recorded for these peptides (Fig. 7c) using a peptide concentration of 20  $\text{ng ml}^{-1}$  (Fig. 7c). After a lag phase of 20 min, zoospores burst progressively reaching a plateau of 10-fold over the control with a lag phase of 40 min (polyamine sulphate) or 80 min (RGD). In contrast, the DGR peptides were found to be mostly ineffective. Dose-response curves assessed at 90 min after addition of the peptides (Fig. 7d) showed a strong increase of burst with increasing concentrations for the RGD peptide, resulting in almost 20-fold higher values compared to control, whereas there was little effect of DGR even at the highest concentration (50  $\text{ng ml}^{-1}$ ). Polyamine sulphate levelled off at a plateau that was around half the value observed for the RGD peptide. These observations indicate that RGD can impair the function of the contractile vacuole. This inhibition is specific, since only a part of this effect can be phenocopied by the unspecific, positively charged polyamine sulphate.

### Glycyrrhizin can inhibit contractile vacuole activity depending on actin and a RboH functional analogue

Since extracts from liquorice (*Glycyrrhiza spec.*) have been reported to be effective against different Oomycete pathogens (Schuster et al. 2010; Scherf et al. 2012), we wondered whether such extracts would affect the activity of the contractile vacuole. For the sake of standardisation, we used a commercial phytotherapeutic extract of *G. uralensis*, a species that is used under the name *Gan Cao* in Traditional Chinese Medicine. We found that even high dilutions were able to induce significant zoospore burst by about 5-fold for a dilution establishing estimated 50 ng ml<sup>-1</sup> of the active compound, glycyrrhizin (Fig. 8a). Likewise, we could induce a similar burst by low concentrations (250 nM) of the membrane rigidifier dimethyl sulfoxide, low concentrations (250 nM) of the actin polymerisation inhibitor Latrunculin B, or low concentrations of diphenylene iodonium (DPI), a flavoprotein inhibitor that in plant cells specifically blocks the NADPH oxidase Respiratory burst oxidase Homologue (RboH). Even extremely low concentrations of DPI (2 nM) were sufficient to produce a more than 10-fold increase of zoospore burst. Interestingly, glycyrrhizin added together with DPI did not increase the incidence of burst, but clearly mitigated the effect of DPI (Fig. 8b). To understand whether the

effect of the *G. uralensis* extract was dependent on the medically active compound in this extract, glycyrrhizin (Fig. 8d), we conducted a dose-response study for zoospore burst over different concentrations of glycyrrhizin in comparison to different concentrations of the extract estimated to establish equivalent concentrations of glycyrrhizin (Fig. 8c). We observed a logarithmical relation for the response over the concentration of glycyrrhizin for a tested dose range of 50 to 5000 ng ml<sup>-1</sup> (corresponding to 61 nM to 6.1 μM of glycyrrhizin). For the extract, there was a dose-dependent increase of burst as well, but this increase was already saturating for an estimated glycyrrhizin concentration of around 500 ng ml<sup>-1</sup> (which would correspond to an estimated concentration of 610 nM of glycyrrhizin) at a level that was reached for pure glycyrrhizin only at a 10-fold higher concentration. This indicates that in the extract, unknown secondary compounds enhance the effect of glycyrrhizin. In summary, a plant extract reported to be effective against Oomycete pathogens was observed to stimulate zoospore burst, and this effect could be mostly (but not exclusively) accounted for by the bioactive compound glycyrrhizin. Furthermore, two factors (*G. uralensis* extract and DPI) that by themselves both stimulate zoospore burst act antagonistically if given in combination, indicative for a role

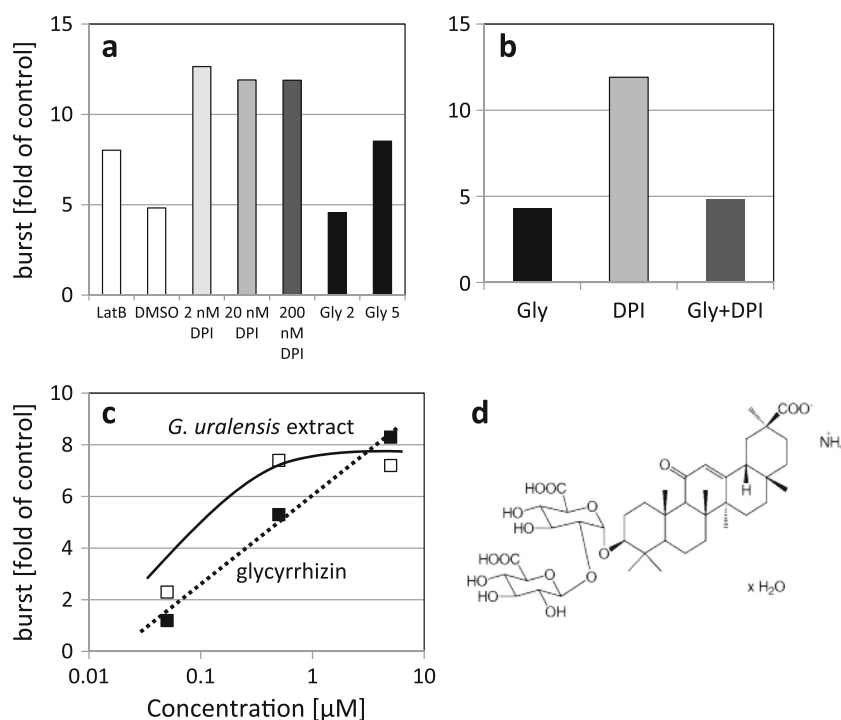


**Fig. 8** Effect of secondary compounds from liquorice (*Glycyrrhiza uralensis*) on zoospore burst. **a** Zoospore burst after 10 min of treatment with a phytotherapeutic extract of *G. uralensis* (Glyc, 20 or 50 ng ml<sup>-1</sup>), compared to the effect of either 250 nM of the actin polymerisation inhibitor Latrunculin B, 250 nM of the membrane rigidifier dimethyl sulfoxide (DMSO), and 2 to 200 nM of

diphenyleneiodonium (DPI), a specific inhibitor of NADPH oxidases, respectively. **b** Antagonistic activity of DPI (20 nM) and the *Glycyrrhiza* extract (20 ng ml<sup>-1</sup>). **c** Dose-response relation of zoospore burst after 10 min of treatment with either an extract of *Glycyrrhiza* (black squares) or the putative active compound glycyrrhizin (grey squares). **d** structure of glycyrrhizin

of membrane-based NADPH oxidases for the regulation of contractile vacuole activity.

## Discussion

The current study was motivated by the search for cellular targets to control the oomycete *P. viticola*, the causative agent of Downy Mildew of Grapevine, as precondition for alternative approaches to conventional fungicides, as well as to the copper preparations that are still widely used in organic viticulture. The contractile vacuole of the zoospores represents a promising target, since even minor perturbation of its functionality will interrupt the infection cycle during a stage, where the pathogen is most vulnerable and accessible to chemical control. We therefore characterised the rise and fall of the contractile vacuole by life cell imaging as well as by ultrastructural investigations. We further probed for the effect of compounds presumably acting on osmosensing, including the plasmalemmal reticulum (RGD peptides), osmotic potential (NaCl), or apoplastic oxidative burst (Cu and Al ions). Our results indicate that the NADPH oxidase in the plasma membrane might be an interesting target, which in the future could be modulated by non-toxic compounds to restrict new infections most efficiently.

**Structural aspects of the contractile vacuole** The contractile vacuole represents the central trait of a larger subcellular structure, the contractile vacuole complex. In its full composition, this complex comprises a network of accessory tubules and vesicles, called spongiome, along with an expulsion pore. However, this complex comes in quite different and variable forms, depending on the respective taxon as comprehensively treated in the classical review by Patterson (1980). In the oomycete *Phytophthora nicotianae*, the relationship between the spongiome and the contractile vacuole (also termed as water expulsion vacuole) has been addressed in more detail using specific antibodies against a vacuolar proton ATPase (Mitchell and Hardham 1999). These antibodies label epitopes in the spongiome and this allowed to ask whether these epitopes would later appear in the water expulsion vacuole or even at the plasma membrane. Such a mechanism had been proposed from experiments involving video microscopy in zoospores of *P. palmivora* (Cho and Fuller 1989). However, the vacuolar proton ATPase was confined to the spongiome and was not seen on the bladder membrane nor on the plasma membrane, suggesting that the spongiome remains a distinct entity and is not incorporated into the water expulsion vacuole. For the oomycete *Saprolegnia*, punctuate clusters of actin surrounding the water expulsion vacuole were visualised by rhodamine phalloidin indicative of actomyosin-based contractility being involved in the expulsion (Heath and Harold

1992). Also in our study, actin in the turgescence sporangia formed punctuate structures as well those that were interconnected by filaments. Although it is tempting to link those with the actin structures around the water expulsion vacuole shown for *Saprolegnia* (Heath and Harold 1992), care is required, because at this stage, the vacuoles are not fully developed, such that the structural context is not clear. Electron microscopy shows a dramatic reorganisation of vesicles in the maturing sporangium (Fig. 2). Numerous grey vesicles are replaced by white and larger vesicles. Transitional stages can be encountered where a grey vesicle is seen inside the white vesicle. At the same time, basal bodies and new membranes separating the individual zoospores are found, while the outer membrane of the individuating syncytium is detached from the sporangial wall. From this, one can conclude that the contribution of the sporangial wall to the intracellular water potential will vanish, such that the water potential should drop dramatically requiring the activity of a water expulsion vacuole. Whether the observed vesicle remodelling is linked with the formation of a contractile vacuole complex is unclear, but the temporal coincidence would be consistent with such a hypothesis.

At the time of zoospore individuation, water expulsion activity commences. Since the activity is still much slower than in the freely swimming zoospores, it is easier to follow the subcellular details. We were particularly interested in a potential membrane flow between spongiome and bladder membrane and used the endomembrane dye DiOC<sub>6</sub> in combination with spinning disc confocal microscopy in zoospores that were preparing to hatch (Fig. 4). During the phase, when the vacuole appeared rough and granular, we observed a star-like ER structure composed of cisternae in the grids separating the chambers of the water-expulsion vacuole. These cisternae coexisted with a rosette-like structures surrounding the site of water release and also showed some continuities with these rosettes. These rosette-like structures might correspond to the multilayered arrays of rough endoplasmic reticulum visualised by electron microscopy to surround the water expulsion vacuole of *Phytophthora* (Hyde et al. 1991). In contrast to this first stage, the ER did not show any link with the vacuole during the next stage, when the vacuole was smooth. What we did not observe was a repartitioning of ER label from the spongiome into the bladder membrane, consistent with the findings obtained by labelling the vacuolar proton ATPase (Mitchell and Hardham 1999). We therefore arrive at a model, where the ER organised in the spongiome is distinct from the ER subtending the vacuole, and where both ER structures persist during expulsion.

**Functional aspects of the contractile vacuole** The activity of the water expulsion vacuole became detectable already several minutes prior to hatching, consistent with reports for *Phytophthora* (Mitchell et al. 2002; Hardham 2005), and then

strongly accelerated after hatching with a cycle of around 3 s, from which we calculated that every 75 s (corresponding to some 25 cycles), the swimming zoospore must expel one entire cell volume of water in order to escape burst. Although the periodically growing and shrinking central bladder covers a significant part of the cell volume, overall, the zoospores do not exhibit obvious changes of shape nor volume. This implies an efficient recycling of membrane material. In fact, already the prehatching zoospores seem to be filled with endosomes, if labelled with the polystyryl dye FM4-64 (Fig. 5b). Also, numerous vesicles could be seen to merge with the vacuole during the granular phase (Fig. 6a; Supplemental Movie S2). Interestingly, this vesicle recycling to the bladder co-exists with a situation, where the spongiome membrane seems to persist as separate entity.

To get insight into cellular and molecular components involved in the activity of the contractile vacuole complex, we probed functionality by measuring the incidence of zoospore burst in response to different ions or specific peptides (Fig. 7). Treatment with low concentrations (<100  $\mu\text{M}$ ) of sodium chloride induced a slight increase of zooplast burst; the effect was saturated from 20  $\mu\text{M}$  NaCl. The osmotic pressure caused by these low concentrations of NaCl is in the range of only 1 Pa, which is five orders of magnitude lower than the turgor pressures usually measured in walled cells, and falls in the range of pressure exerted by Brownian movement (thermal noise). Moreover, the salt should cause a decrease of water potential in the apoplast rather than in the cytoplasm. This suggests that NaCl acts as a signal rather than as a bulk component. In plant cells, uptake of sodium ions through non-selective cation channels rapidly stimulates apoplastic oxidative burst by membrane located NADPH oxidases (reviewed in Ismail et al. 2014). A role of a signalling function is also supported by the effect of aluminium and copper ions, which stimulate zoospore burst very efficiently at very low (again micro molar range) concentrations. Both compounds have been used against Oomycete pathogens (e.g. Dercks and Buchenauer 1987 for aluminium, e.g. Dagostin et al. 2011 for copper), but their mode of action has remained far from clear, although copper has been used since the mid-nineteenth century in viticulture. Due to their incompletely filled  $\delta$ -orbital, these ions readily trigger Fenton type reactions resulting in superoxide ions (Schützendübel and Polle 2002). For plant cells, apoplastic superoxide accumulation in response to copper has been demonstrated to activate phospholipase D-dependent signalling, which activates a NADPH oxidase and thus amplifies apoplastic oxidative burst (Yu et al. 2008). To what extent this NADPH oxidase-dependent signalling loop is present in Oomycetes remains to be elucidated, but to assume the NADPH oxidase as a common link in the mode of action

for these three ions would at least provide an attractive hypothesis, worth to be tested further.

A role of the NADPH oxidase is also supported by a surprising result observed while probing the effect of glycyrrhizin (Fig. 8). In higher plants, the NADPH oxidase is functionally integrated with superoxide and membrane bound actin in a self-amplifying loop (Eggenberger et al. 2017) that seems to balance auxin-dependent growth and stress responses triggered by perturbations of membrane integrity. Here, perturbations of membrane integrity cause a bundling of cortical actin filaments, and this actin-bundling can be suppressed by diphenylene iodonium chloride (DPI), a specific inhibitor of the NADPH oxidase. Interestingly, DPI alone can induce actin bundling as well. Thus, two factors that cause actin bundling, if given alone, neutralise each other, if administered in combination. This very specific (and somewhat counter-intuitive) aspect is mirrored in the zoospore burst: While glycyrrhizin, if given alone, induces zoospore burst (Fig. 8c), it can mitigate the burst induced by DPI (Fig. 8b). That actin is involved in contractility, is seen in the induction of burst by low (250 nM) concentrations of Latrunculin B, and is also predicted from the association of actin with the contractile vacuole (Heath and Harold 1992); further, membrane fluidity might be required, since as little as 250 nM of DMSO can induce some burst as well.

While an oxidative burst (possible interfering with actin functionality) might account for the induction of zoospore burst by metal ions, the effect of RGD peptides seems to act on a different target. Although these peptides are not expected to permeate the membrane, they can induce strong remodelling of the cytoplasmic architecture (Canut et al. 1998), probably targeting on membrane-bound actin (reviewed in Baluška et al. 2003, Pickard 2008). This effect is specific, because a peptide with inverted sequence (DGR peptide) is effective only at much higher concentrations, possible through positive charges in the sequence, because polyamines can induce some burst as well (Fig. 7), although saturating at an amplitude which is only half of that achieved by the RGD peptides. Whether integrin-like proteins are to be expected in Oomycetes, is an open question, but biochemical and genomic evidence in prasinophytes support scenarios on algal evolution (Becker et al. 2015), where the original cell surface of the primary zoo flagellate host (presumably harbouring integrin-like proteins) has been progressively complemented into the cellulosic cell wall typical for plants. Irrespective of the admittedly speculative presence of integrin-like proteins, the specific effect of RGD peptides on zooplast burst might be caused by a detachment of membrane-associated actin impairing the functionality of the contractile vacuole complex.

**Outlook: Towards environmentally friendly alternatives to copper** In organic viticulture, copper preparations are currently used as one of the few alternatives to the

conventional fungicides. This practice is highly problematic, because copper will become enriched in the soil. In fact, the traditional use of so called Bordeaux mixtures has left already a negative footprint with copper contents that are up to 10-fold higher in vineyard soils compared to other agricultural systems (Brun et al. 1998). Environmentally friendly alternatives are therefore highly demanded. While the effect of RGD peptides is specific, application of these peptides in agriculture is currently still far from economic feasibility. Secondary plant compounds might be more promising. In fact, extracts from plants had been screened for inhibitory effects upon *P. viticola* and several extracts had been reported to be bioactive (Chen et al. 2002). However, field studies are still rare. A systematic study on extracts from common sage (*Salvia officinalis*) against *P. viticola* in grapevine (Dagostin et al. 2010) yielded promising results, but the rain fastness of these extract was found to be limiting. The jellifying ability of liquorice extracts might be of special interest in this respect. In fact, liquorice extracts were already positively tested in the control of Oomycetes affecting vegetables such as cucumber (Schuster et al. 2010, Scherf et al. 2012). Since liquorice can be produced in considerable quantities and is also used in veterinary medicine (for instance to cure digestive imbalance in horses), a combination with interactive prediction systems already in use for Downy Mildew (Bleyer et al. 2011) has some potential for an environmentally safe pathogen control expanding the toolbox for antifungal plant-extracts, such as saponins or primrose extracts used as strategy against black rot (Koch et al. 2013). It should be noted that such a strategy would not arise from a high-throughput screen of chemical libraries, but from detailed knowledge on the Achilles' Heel of a pathogen, i.e. from hypothesis-driven research.

**Acknowledgements** We gratefully acknowledge Joachim Daumann and Kerstin Huber (Botanical Garden of the Karlsruhe Institute of Technology) for efficient support with the plant material. Also, we acknowledge Prof. Dr. Otmar Spring and Dr. Javier Gómez (University of Hohenheim) for kindly providing single-sporangia strains of *P. viticola*. This work was supported by the VITIFUTUR Interreg V Upper Rhine project co-financed by the European Union/European Regional Development Fund (ERDF) and the German Federal Agency for Agriculture (Programme for Sustainable Agriculture, BÖLN).

#### Compliance with ethical standards

**Funding** This study was supported by funds from the BACCHUS Interreg IV Upper Rhine project co-financed by the European Union/European Regional Development Fund (ERDF) and the German Federal Agency for Agriculture (Programme for Sustainable Agriculture, BÖLN).

**Conflict of interest** The authors declare that they have no conflict of interest.

## References

- Allen RN, Newhook FJ (1973) Chemotaxis of zoospores of *Phytophthora cinnamomi* to ethanol in capillaries of soil pore dimensions. *Transact Brit Mycol Soc* 61:287–302
- Baluška F, Šamaj J, Wojtaszek P, Volkmann D, Menzel D (2003) Cytoskeleton plasma membrane-cell wall continuum in plants. Emerging links revisited. *Plant Physiol* 133:482–491
- Bartlett DW, McClough J, Godwin JR, Hall AA, Hamer M, Parr-Dobrzanski B (2002) Thestrobilurin fungicides. *Pest Manag Sci* 58:649–662
- Beakes GW, Glocklin SL, Sekimoto S (2012) The evolutionary phylogeny of the oomycete “fungi”. *Protoplasma* 249:3–19
- Becker B, Doan JM, Wustman B, Carpenter EJ, Chen L, Zhang Y, Wong GK-S, Melkonian M (2015) The origin and evolution of the plant cell surface: algal integrin-associated proteins and a new family of integrin-like cytoskeleton-ECM linker proteins. *Genome Biol Evolution* 7:1580–1589
- Bleyer G, Kassemeyer H-H, Breuer M, Krause R, Viret O, Dubuis P. H, Fabre A.L, Bloesch B, Siegfried W, Naef A, Huber M (2011) “VitiMeteo”—a future-oriented forecasting system for viticulture. *IOBC/Wprs Bulletin* 67:69–77
- Brun LA, Maillat J, Richarte J, Herrmann P, Remy JC (1998) Relationships between extractable copper, soil properties and copper uptake by wild plants in vineyard soils. *Environ Pollut* 102:151–161
- Canut H, Carrasco A, Galaud JP, Cassan C, Bouyssou H, Vita N, Ferrara P, Pont-Lezica R (1998) High affinity RGD-binding sites at the plasma membrane of *Arabidopsis thaliana* links the cell wall. *Plant J* 16:63–71
- Chen HR, Sheu SJ (1993) Determination of glycyrrhizin and glycyrrhetic acid in traditional Chinese medicinal preparations by capillary electrophoresis. *J Chromatogr A* 29:184–188
- Chen J, Dai G, Gu Z, Miao Y (2002) Inhibition effect of 58 plant extracts against grape downy mildew (*Plasmopara viticola*). *Natural Product Res Development* 14:9–13
- Chen WJ, Delmotte F, Richard-Cervera S, Douence L, Greif C, Corio-Costet MF (2007) At least two origins of fungicide resistance in grapevine downy mildew populations. *Appl Environm Microbiol* 73:5162–5172
- Chitcholtan K, Garrill A (2005) A beta4 integrin-like protein co-localises with a phosphotyrosine containing protein in the oomycete *Achlya bisexualis*: inhibition of tyrosine phosphorylation slows tip growth. *Fung Genet Biol* 42:534–545
- Cho CW, Fuller MS (1989) Observations of the water expulsion vacuole of *Phytophthora palmivora*. *Protoplasma* 149:47–55
- Dagostin S, Formolo T, Giovannini O, Pertot I, Schmitt A (2010) *Salvia officinalis* extract can protect grapevine against *Plasmopara viticola*. *Plant Dis* 94:575–580
- Dagostin S, Schärer HJ, Pertot I, Tamm L (2011) Are there alternatives to copper for controlling grapevine downy mildew in organic viticulture? *Crop Prot* 30:776–788
- Dercks W, Buchenauer H (1987) Comparative studies on the mode of action of aluminium ethyl phosphite in four *Phytophthora* species. *Crop Prot* 6:82–89
- Eggenberger K, Sanyal P, Hundt S, Wadhvani P, Ulrich AS, Nick P (2017) Challenge integrity: the cell-permeating peptide BP100 interferes with the actin-auxin oscillator. *Plant Cell Physiol* 58:71–85
- Eibach R, Zyprian E, Welter L, Töpfer R (2007) The use of molecular markers for pyramiding resistance genes in grapevine breeding. *Vitis* 46:120–124
- Gay JL, Greenwood AD, Heath IB (1971) The Formation and Behaviour of Vacuoles (Vesicles) during Oosphere Development and Zoospore Germination in Saprolegnia. *Microbiology* 65:233–241

- Gessler C, Pertot I, Perazzolli M (2011) *Plasmopara viticola*: a review of knowledge on downy mildew of grapevine and effective disease management. *Phytopathol Mediterr* 50:3–44
- Giraud F, Molitor D, Bleunven M, Evers D (2013) Fungicide sensitivity profiles of the *Plasmopara viticola* populations in the Luxembourgian grape-growing region. *J Plant Pathol* 51:55–62
- Gómez-Zeledón J, Zipper R, Spring O (2013) Assessment of phenotypic diversity of *Plasmopara viticola* on *Vitis* genotypes with different resistance. *Crop Prot* 54:221–228
- Hardham AR (2005) *Phytophthora cinnamomi*. *Mol Plant Pathol* 6:589–604
- Heath IB, Harold RL (1992) Actin has multiple roles in the formation and architecture of zoospores of the oomycetes, *Saprolegnia ferax* and *Achlya bisexualis*. *J Cell Science* 102:611–627
- Heumann HG (1992) Microwave-stimulated glutaraldehyde and osmium tetroxide fixation of plant tissue: ultrastructural preservation in seconds. *Histochemistry* 97:341–347
- Hostetter MK (2000) RGD-mediated adhesion in fungal pathogens of humans, plants and insects. *Current Op Microbiol* 3:344–348
- Hyde GJ, Hardham AR (1993) Microtubules regulate the generation of polarity in zoospores of *Phytophthora cinnamomi*. *Eur J Cell Biol* 62:75–85
- Hyde GJ, Lancelle S, Hepler PK, Hardham AR (1991) Freeze substitution reveals a new model for sporangial cleavage in *Phytophthora*, a result with implications for cytokinesis in other eukaryotes. *J Cell Sci* 100:735–746
- Ismail A, Takeda S, Nick P (2014) Life and death under salt stress: same players, different timing? *J Exp Bot* 65:2963–2979
- Jürges G, Kassemeyer H-H, Dürrenberger M, Düggelin M, Nick P (2009) The mode of interaction between *Vitis* and *Plasmopara viticola* Berk. & Curt. Ex de Bary depends on the host species. *Plant Biol* 11:886–898
- Kaminskyj SG, Heath IB (1995) Integrin and spectrin homologues, and cytoplasm-wall adhesion in tip growth. *J Cell Sci* 108:849–856
- Kiefer B, Riemann M, Büche C, Kassemeyer HH, Nick P (2002) The host guides morphogenesis and stomatal targeting in the grapevine pathogen *Plasmopara viticola*. *Planta* 215:387–393
- Kleinig H, Sitte P (1986) *Zellbiologie—ein Lehrbuch*. Gustav-Fischer, Stuttgart-New York
- Koch E, Enders M, Ullrich C, Molitor D, Berkelmann-Löhnertz B (2013) Effect of *Primula* root and other plant extracts in infection structure formation of *Phyllosticta ampellicida* (asexual stage of *Guignardia bidwellii*) and on black rot disease of grapevine in the greenhouse. *J Plant Diseases Protection* 120:26–33
- Koning AJ, Lum PY, Williams JM, Wright R (1993) DiOC<sub>6</sub> staining reveals organelle structure and dynamics in living yeast cells. *Cell Mot Cytoskelet* 25:111–128
- Kortekamp A (2003) Leaf surface topography does not mediate tactic response of *Plasmopara*-zoospores to stomata. *J Applied Bot* 77:41–46
- Kutschera U, Hossfeld U (2012) Physiological phytopathology—origin and evolution of a scientific discipline. *J Appl Bot* 85:1–5
- Liu Q, Qiao F, Ismail A, Chang X, Nick P (2013) The plant cytoskeleton controls regulatory volume increase. *BBA Membranes* 1828:2111–2120
- Mitchell HJ, Hardham AR (1999) Characterisation of the water expulsion vacuole in *Phytophthora nicotianae* zoospores. *Protoplasma* 206:118–130
- Mitchell HJ, Kovac KA, Hardham AR (2002) Characterisation of *Phytophthora nicotianae* zoospore and cyst membrane proteins. *Mycol Res* 106:1211–1223
- Müller K, Sleumer H (1934) Biologische Untersuchungen über die Peronosporakrankheit des Weinstockes mit besonderer Berücksichtigung ihrer Bekämpfung nach der Inkubationskalendermethode. *Landwirtschaftl Jahrb Z Wissenschaftl Landwirtschaft* 79:509–576
- Nick P (2011) Mechanics of the cytoskeleton. In: Wojtaszek P (ed) *Mechanical integration of plant cells and plants*. Springer, Berlin-Heidelberg, pp 53–90
- Patterson DJ (1980) Contractile vacuoles and associated structures: their organization and function. *Biol Rev* 55:1–46
- Pickard BG (2008) “Second extrinsic organizational mechanism” for orienting cellulose: modeling a role for the plasmalemmal reticulum. *Protoplasma* 233:7–29
- Riemann M, Büche C, Kassemeyer HH, Nick P (2002) Microtubules and actin microfilaments guide the establishment of cell polarity during early development of the wine pathogen *Plasmopara viticola*. *Protoplasma* 219:13–22
- Rouxel M, Mestre P, Comont G, Lehman BL, Schilder A, Delmotte F (2013) Phylogenetic and experimental evidence for host-specialized cryptic species in a biotrophic oomycete. *New Phytol* 197:251–263
- Ruoslahti E (1996) RGD and other recognition sequences for integrins. *Annu Rev Cell Develop Biol* 12:697–715
- Schaubschläger WM, Becker G, Mazur G, Gödde M (1994) Occupational sensitization to *Plasmopara viticola*. *J Allergy Clinical Immunol* 93:457–463
- Scherf A, Treutwein J, Kleeberg H, Schmitt A (2012) Efficacy of leaf extract fractions of *Glycyrrhiza glabra* L. against downy mildew of cucumber (*Pseudoperonospora cubensis*). *Eur J Plant Pathol* 134:55–762
- Schuster C, Konstantinidou-Doltsinis S, Schmitt A (2010) *Glycyrrhiza glabra* extract protects plants against important phytopathogenic fungi. *Commun Agric Appl Biol Sci* 75:531–540
- Schützendübel A, Polle A (2002) Plant responses to abiotic stresses: heavy metal-induced oxidative stress and protection by mycorrhization. *J Exp Bot* 53:1351–1365
- Van Zwieten M, Stovold G, Van Zwieten L (2004) Literature review and inventory of alternatives to copper for disease control in the Australian organic industry. A report for the Rural Industries Research and Development Corporation. RIRDC Project DAN-208A. ISBN 0 7347 1590 0
- Williams MG, Magarey PA, Sivasithamparam K (2007) Effect of temperature and light intensity on early infection behaviour of a Western Australian isolate of *Plasmopara viticola*, the downy mildew pathogen of grapevine. *Austral Plant Pathol* 36:325–331
- Yokozawa T, Liu ZW, Chen CP (2000) Protective effects of *Glycyrrhizae radix* extract and its compounds in a renal hypoxia (ischemia)-reoxygenation (reperfusion) model. *Phytomedicine* 6:439–445
- Yu ZL, Zhang JG, Wang XC, Chen J (2008) Excessive copper induces the production of reactive oxygen species, which is mediated by phospholipase D, nicotinamide adenine dinucleotide phosphate oxidase and antioxidant systems. *J Integr Plant Biol* 50:157–167
- Zaban B, Maisch J, Nick P (2013) Dynamic actin controls polarity induction de novo in protoplasts. *J Integr Plant Biol* 55:142–159